

Path Selection under Budget Constraints in Multihop Cognitive Radio Networks

Miao Pan, *Member, IEEE*, Hao Yue, *Student Member, IEEE*,
Chi Zhang, *Member, IEEE*, and Yuguang Fang, *Fellow, Member IEEE*

Abstract—Cognitive radio (CR) technology opens the licensed spectrum bands for opportunistic usage and initiates spectrum trading to improve the spectrum utilization. In this paper, we investigate the path selection problem in multihop cognitive radio networks (CRNs) under constraints on flow routing, link scheduling and CR source's budget. We extend the per-user-based spectrum trading in prior work to CR session-based spectrum trading, and effectively develop the spectrum trading mechanisms based on the cross-layer optimization in multihop CRNs. We introduce a new service provider, called *secondary service provider* (SSP), to help CR sessions to select the paths for packet delivery. Considering the price of bands and the potential returning of primary services at different CR links, the SSP purchases the licensed spectrum and jointly conducts flow routing and link scheduling under the budget constraints. We also propose a 4D conflict graph to characterize the conflict relationship among CR links and mathematically formulate the path selection problem under multiple constraints into an optimization problem with the objective of maximizing the end-to-end throughput. Due to the NP-hardness of the problem, we have also developed a heuristic algorithm to find the approximate solution.

Index Terms—Cognitive radio networks, uncertain spectrum supply, link scheduling, multihop multipath routing, optimization

1 INTRODUCTION

NOWADAYS, more and more people, families, and companies rely on wireless services for their daily life and business, which leads to a booming growth of various wireless networks and a dramatic increase in the demand for radio spectrum. In parallel with that, current static spectrum allocation policy of Federal Communications Commission (FCC) [1], [2], [3] results in the exhaustion of available spectrum, while a lot of licensed spectrum bands are extremely underutilized. Experimental tests in academia [4], [5] and measurements conducted in industries [6], [7] both show that even in the most crowded region of big cities (e.g., Washington, DC, Chicago, New York City, etc.), many licensed spectrum bands are not used in certain geographical areas and are idle most of the time. Those studies spur the FCC to open up licensed spectrum bands and pursue new innovative technologies to encourage dynamic use of the underutilized spectrum [1]. As one of the most promising solutions, cognitive radio (CR) technology releases the spectrum from shackles of authorized licenses, and enables the CR users to opportunistically utilize the vacant licensed spectrum bands in either temporal or spatial domain.

The idea of opportunistic using licensed spectrum in multihop cognitive radio networks (CRNs) has initiated the

market of spectrum trading and promoted a bunch of interesting research on related topics. Specifically, in [8], Grandblaise et al. generally describe the potential scenarios and introduce some microeconomics inspired mechanisms for opportunistic spectrum accessing, and in [9], Sengupta and Chatterjee propose an economic framework for opportunistic spectrum accessing to guide the design of dynamic spectrum allocation algorithms as well as service pricing mechanisms. From the view of system design, models in game theory, by Wang et al. [10], [11], Pan et al. [12], and Zhang and Zhang [13], and auction designs in microeconomics by Zhou et al. [14], [15], Jia et al. [16], and Wu et al. [17], are exploited to construct the spectrum trading mechanisms with desired properties, such as power efficiency, allocation fairness, incentive compatibility, Pareto efficiency, and so on. From the view of the primary users, Xing et al. [18] and Niyato et al. [19], [20] have well investigated the spectrum pricing issues in the spectrum market, where multiple primary users, whose goal is to maximize the monetary gains with their vacant spectrum, compete with each other to offer spectrum access to the CR users. From the view of the CR users, Pan et al. [21], [22], [23], and [24] have addressed how the CR users optimally distribute their traffic demands over the spectrum bands to reduce the risk for monetary loss, when there is more than one unoccupied licensed band.

Unfortunately, most existing work assume per-user-based spectrum trading (i.e., each CR user purchases available bands from primary users and uses the purchased spectrum for communications), which confronts those mechanisms with several critical problems when they are deployed in multihop CRNs. For instance, it is not clear whom a CR user communicates with (i.e., the CR receiver is not explicitly specified); it is not clear how to find a common band between two CR users to establish communications; it is not clear what kind of quality of service (e.g., throughput, delay, rate, or bandwidth requirement, etc.)

• M. Pan is with the Department of Computer Science, Texas Southern University, 122 Nabrit Science Center, Houston, Texas 77004. E-mail: panm@tsu.edu.

• H. Yue and Y. Fang are with the Department of Electrical and Computer Engineering, University of Florida, PO Box 116130, New Engineering Building, Gainesville, FL 32611-6130. E-mail: {hyue, fang}@ece.ufl.edu.

• C. Zhang is with the School of Information Science and Technology, University of Science and Technology of China, 421 the 4th Electrical Building, Hefei, Anhui 230027, China. E-mail: chizhang@ustc.edu.cn.

Manuscript received 21 May 2011; revised 22 Dec. 2011; accepted 16 Mar. 2012; published online 28 Mar. 2012.

For information on obtaining reprints of this article, please send e-mail to: tmc@computer.org, and reference IEEECS Log Number TMC-2011-05-0272. Digital Object Identifier no. 10.1109/TMC.2012.85.

can be supported. Besides, although some of prior spectrum trading designs consider the impact of frequency reuse [12], [14], [15], [17], they ignore almost all the other factors, e.g., activities of primary services, link scheduling, route selection, and so on, which may significantly affect the performance of CR sessions in multihop CRNs.

Instead of working on per-user-based spectrum trading, in this paper, we investigate the session-based spectrum trading. Suppose that the CR source has a fixed budget and prices for opportunistic spectrum accessing are different for different licensed bands or for the same band at different locations. Given a CR session and multiple routes between the CR source and destination, we endeavor to find a path with the maximum end-to-end throughput under the CR source's budget in multihop CRNs. To achieve this objective, we have to consider the price of the bands, budget constraints of CR source, link scheduling constraints, flow routing constraints, and possible returning of primary services, when selecting the path as well as the licensed bands for opportunistic accessing. In this paper, we mathematically formulate these concerns into an optimization problem and provide near-optimal solutions using linear programming. We also propose a heuristic algorithm to give feasible solutions to the path selection problem under multiple constraints. Our contributions are summarized as follows:

- We introduce a novel service provider for CR users, called *secondary service provider* (SSP), into the network and employ SSP to help the CR session select the path for packet delivery. On behalf of the CR links, the SSP purchases licensed bands from primary users for CR nodes' opportunistic spectrum accessing w.r.t. the price of the bands as well as the activities of primary services. Meanwhile, the SSP seeks the maximum throughput route for the CR session by conducting link scheduling and path selection under the budget of CR source.
- Inspired by the link conflict graph in single-radio single-channel (SR-SC) networks [25], [26] and the 3D conflict graph in multiradio multichannel (MR-MC) networks [27], we propose a 4D conflict graph to describe the conflict relations among CR links in competing for bands w.r.t. the price of bands and the probability of primary services' returning in multihop CRNs. Similar to the methodology used in [27], we interpret each vertex in the graph as a basic resource point for scheduling. Furthermore, we represent each resource point with a *link band probability price* (LBP²) quadruplet and construct the 4D conflict graph consisting of LBP² quadruplets.
- Based on the 4D conflict graph, the SSP can mathematically formulate the path selection as a joint routing and link scheduling optimization problem under the CR source's budget constraint. Given all the independent sets in CRNs, the SSP can relax the integer variables in the formulation, solve the optimization problem by linear programming and find the optimal path with the largest end-to-end throughput between CR source and destination.
- It is NP-hard to find all the independent sets in CRNs [28]. It is even too complicated for the SSP to

find all independent sets of a given path if the number of links or the available licensed bands is large. Therefore, we develop a heuristic algorithm to deal with the path selection problem using local conflict cliques of LBP² quadruplets. We let the SSP layer the 4D conflict graph by the number of licensed bands, switch LBP² quadruplets to mitigate the co-band interference, and leverage the conflict cliques to find the optimal path with the largest path capacity considering the CR source's budget.

- By carrying out simulations, we demonstrate the impact of the CR source's budget, the number of available bands, and the distance between the CR source and destination on the performance of path selection in CRNs. We also compare the path selection algorithms including the optimal path selection, the proposed heuristic path selection and the single-band-based path selection proposed in [26], and show that the heuristic algorithm is much better than the single-band-based one, and is close to the optimal one in terms of the path capacity.

The rest of the paper is organized as follows: in Section 2, we review related work on cross-layer optimization for SR-SC and MR-MC networks and state of the art on CRNs. In Section 3, we introduce the spectrum market and related models in multihop CRNs. In Section 4, we describe the 4D conflict graph and present the concept of independent sets and conflict cliques in 4D conflict graph. In Section 5, we mathematically describe scheduling and routing constraints in multihop CRNs, formulate the path selection under multiple constraints into an optimization problem and solve it by linear programming. In Section 6, we develop a heuristic algorithm for the high throughput path selection. Finally, we conduct simulations and analyze the performance results in Section 7, and draw concluding remarks in Section 8.

2 RELATED WORK

How to find the path with the largest end-to-end throughput under joint link scheduling and routing constraints has been extensively studied in both SR-SC networks and MR-MC networks. Jain et al. [29] studied the impact of interference on performance of multihop wireless network based on an NP-hard optimization problem. Zhai and Fang [26] investigated the path capacity of a given path considering link scheduling and leveraged the interference clique transmission time to design a routing metric for high-throughput path selection in SR-SC networks. In [25], Chen et al. extended this work to multirate SR-SC networks, and addressed how to find a path with high available bandwidth considering both the interference from background traffic and that along the path. In MR-MC networks, Li et al. [27] proposed a 3D (i.e., *radio-link-channel*) conflict graph and exploited it to efficiently solve the optimal path capacity problem using linear programming.

However, different from the mobile device with a single radio in SR-SC networks or the one with multiple radios in MR-MC networks, the CR device has only one radio but the radio is a software defined one [1], [2], [3], which is

supposed to switch frequencies across a wide spectrum range (i.e., from 20 MHz to 2.5 GHz [30], [31], [32]). Besides, the opportunistic spectrum usage of the CR users closely depends on the activities of primary services. The limitations in CR hardware and the impact of primary users make the path selection problem much more complex in CRNs than that in SR-SC networks and MR-MC networks.

In CR research community, there have been some efforts devoted to cross-layer optimization as well. Tang et al. [33] studied the joint spectrum allocation and link scheduling problems with the objectives of maximizing throughput and achieving certain fairness in CRNs. Hou et al. [34] investigated the joint frequency scheduling¹ and routing problem with the objective of minimizing the network-wide spectrum resource and presented a centralized algorithm for spectrum sharing in CRNs. In their following work, Shi and Hou [35] also provided a distributed approach to address this issue. Considering the uncertain spectrum supply, Pan et al. [21], [22], and [36] proposed to model the vacancy of licensed bands as a series of random variables, characterized the multihop CRNs with a pair of (α, β) parameters and minimized the usage of licensed spectrum to support CR sessions with rate requirements at certain confidence levels.

In the existing literature of multihop CRNs, there remains a lack of study on the path selection problem by jointly considering routing and link scheduling. Meanwhile, there is a lack of bond to connect the research on spectrum trading and the research on cross-layer optimization in multihop CRNs.

Our work bridges the gap between these two active research topics, i.e., spectrum trading mechanism design and cross-layer optimization, in multihop CRNs. We have a comprehensive study on the path selection problem considering multiple factors including the price of the bands, budget constraints of CR source, link scheduling constraints, flow routing constraints, and activities of primary services. This work extends the per-user-based spectrum trading into session-based spectrum trading and makes those microeconomics inspired spectrum trading mechanisms practically applicable in multihop CRNs.

3 NETWORK MODEL

3.1 Spectrum Market and Opportunistic Spectrum Accessing

We consider a spectrum market in multihop CRNs [19], [21], [22], [23], [24] consisting of multiple primary users operating on different frequency bands and an SSP (e.g., a base station (BS) or an access point (AP)) who serves a group of CR users $\mathcal{N} = \{1, 2, \dots, n, \dots, N\}$. Suppose that the set of licensed spectrum bands $\mathcal{B} = \{1, 2, \dots, b, \dots, B\}$ have the identical bandwidth, where the size of the bandwidth is equal to 1. We also assume that a CR user has only one radio, but the radio can be tuned into any available frequency band for packet delivery, i.e., a CR user can only work on one of the available bands at one time. As shown in Fig. 1, some spectrum bands at certain geographical locations (the bands fully in shade) may be reserved

1. In this paper, frequency scheduling refers to the scheduling in frequency domain or means frequency band allocation, and link scheduling refers to the scheduling in time domain.

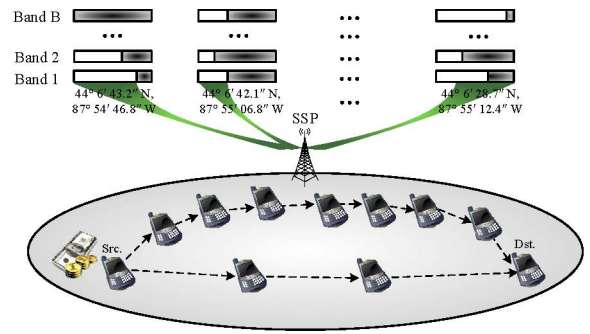


Fig. 1. Spectrum market and opportunistic spectrum accessing for packet delivery under CR source's budget constraints in multihop CRNs.

for the exclusive usage of specific primary services (e.g., restricted areas for military use or public safety, danger areas of emergency or disaster, etc.); some other licensed bands (the bands partially in shade) are opened and the “white space” is available for opportunistic accessing of CR users. To put it in a mathematical way, let $\mathcal{B}_i \subseteq \mathcal{B}$ represent the set of available licensed bands at CR node $i \in \mathcal{N}$. \mathcal{B}_i may be different from \mathcal{B}_j , where j is not equal to i , and $j \in \mathcal{N}$, i.e., possibly $\mathcal{B}_i \neq \mathcal{B}_j$.

In this case, primary users will set reasonable prices for the available licensed bands considering the unpredictable activities of the primary services as well as competition among primary users in the spectrum market [16], [18], [19], and sell those bands for monetary gains. Besides, we assume the spectrum trading takes place periodically, where the duration of a trading period is τ , and the payment for spectrum trading is nonrefundable.² Instead of being the trading proxy for CR users [9], the SSP plays the role of trading proxy for CR sessions. Suppose there is a unicast CR session in CRNs. Let s_r/d_t denote the source/destination CR node of this session, and E be the budget of the CR source s_r . To forward packets to the destination, the source CR node³ must pay for the opportunistic spectrum usage of the CR links along the selected path to primary users via the SSP. Meanwhile, the availability of the purchased bands is not guaranteed. CR links can opportunistically use the purchased licensed bands when the primary services are not on, but have to stop using those bands when primary services become active. Given such a CR session, in this work, the SSP collectively harvests licensed spectral resource, purchases spectrum bands for CR links at different locations, and jointly conduct link scheduling and route selection under the budget constraints with the objective of maximizing the end-to-end throughput.⁴

3.2 Other Related Models in CRNs

3.2.1 Probability Model of Primary Services

It is necessary to model the activities of primary services because the transmissions of a CR link over band $b \in \mathcal{B}$

2. The trading period τ should not be too long (e.g., months or years) to make dynamic spectrum access infeasible, and it should not be too short (e.g., milliseconds or seconds) to incur overwhelming overhead in spectrum trading. The typical duration is minutes or hours as shown in [37]. In the rest of paper, we assume that τ is of fixed duration, so that the time parameter is not included in our formulation.

3. Incentive issues of the relay CR nodes are not considered in this paper.

4. By exchanging small-size control messages with the CR users over the dedicated channel (e.g., cognitive pilot channel), the SSP can conduct the spectrum trading and schedule the transmissions of large-size data packets for multihop CR communications.

closely depend on the availability of band b . As shown in [38], [39], and [40], the traffic of primary services can be modeled as a two state ON-OFF process, where an ON state represents the band is occupied by primary services, and an OFF state represents the band is available for CR users' opportunistic accessing. Let q_{ij}^b represent the probability that the band b at link l_{ij} is in OFF state, and $(1 - q_{ij}^b)$ represent the probability that the band b at link l_{ij} is in ON state, where $b \in \mathcal{B}_i \cap \mathcal{B}_j$.

3.2.2 Transmission/Interference Range

The interference in wireless networks can be defined according to the protocol model or the physical model [41]. Suppose all CR nodes use the same power for transmission. Then, in protocol model [26], [41], there will be a fixed transmission range and a fixed interference range, where the interference range is typically two or three times of the transmission range. These two ranges may vary with the frequency bands. The conflict relationship between two links over the same band can be determined by the specified interference range. The protocol model is adopted by most of the existing work [26], [27], [33], [34], [36], by which the interference over a network can be abstracted into a conflict graph. We also exploit the protocol model to characterize the interference relationship among CR links in this research, and extend the conflict graph into 4D conflict graph considering the features of spectrum trading in CRNs, which will be described in the next section. In addition, if we properly set the interference range, we can accurately transform a protocol model into a physical model as illustrated in [42].

4 4D CONFLICT GRAPH, CONFLICT CLIQUES, AND INDEPENDENT SETS IN MULTIHOP CRNs

To pursuit high end-to-end throughput or path capacity, it is necessary for the SSP to jointly consider flow routing and link scheduling. To effectively schedule data transmission among different CR links, it is necessary for the SSP to find the independent sets in the conflict graph constructed from CRNs [25], [26]. In this section, we extend the conflict graph to multidimension case and establish a 4D conflict graph to characterize the interference relation among CR links. In the background of 4D conflict graph, we also redefine independent sets and conflict cliques, which can help the SSP make decisions of licensed-band purchasing, spectrum assignment, link scheduling, and flow routing under the budget constraints in multihop CRNs.

4.1 Construction of the 4D Conflict Graph

Regarding the unpredictable activities of primary services and the features of CR transceivers, we introduce a 4D conflict graph to characterize the interference relationship among CR links in CRNs. Specifically, we interpret a CRN as a 4D resource space, with dimensions defined by links, bands, the probability that the band is available for OSA and the charging price. In parallel with this, in a 4D conflict graph $\mathcal{G}(\mathcal{V}, \mathcal{E})$, each vertex corresponds to an LBP² price quadruplet, where an LBP² quadruplet is defined as

$$\text{link-band-probability-price} : (l_{ij}, b, q_{ij}^b, p_{ij}^b).$$

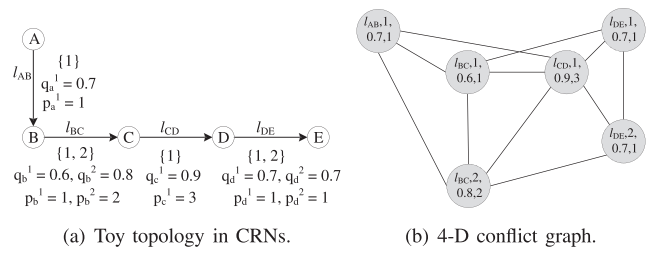


Fig. 2. Conflict relationship represented by 4D conflict graph in CRNs.

The LBP² quadruplet indicates that the CR link l_{ij} ($i, j \in \mathcal{N}$) operates on band b w.r.t the activities of the primary services over this link. The availability of band b at link l_{ij} is denoted by q_{ij}^b and the price charged for l_{ij} 's opportunistic use of band b is represented by p_{ij}^b . According to the definition of LBP² quadruplets, we can enumerate all combinations of CR users, bands, the availability of bands and the price of bands, which can potentially enable a CR communication link.

Obviously, the conflict relationship among LBP² quadruplets in CRNs is more complex than that among links in SR-SC networks, and that among link-channel pairs in MR-MC networks. Two quadruplets are said to interfere with each other if either of the following two conditions holds:

- *Condition 1.* Two different LBP² quadruplets have one or two CR nodes in common.
- *Condition 2.* If two different LBP² quadruplets are using the same band, the receiving CR node of one LBP² quadruplet is within the interference range of the transmitting CR node in the other LBP² quadruplet.

Based on these conditions, we connect two vertices in \mathcal{V} with an undirected edge in $\mathcal{G}(\mathcal{V}, \mathcal{E})$, if their corresponding LBP² quadruplets interfere with each other.

For illustrative purpose, we take a simple example to show how to construct a 4D conflict graph. In this toy CRNs in Fig. 2a, we assume there are five CR users with CR transceivers, i.e., A, B, C, D, and E, and two licensed bands, i.e., band 1 and band 2. Depending on the geographic locations, the set of currently available frequency bands at one CR link may not be the same as that at another CR link as mentioned in Section 3.1. For example, the currently available band set for link l_{AB} is $\{1\}$ and the band set for link l_{BC} is $\{1, 2\}$. Meanwhile, the CR transmissions are subject to the unpredictable returning of primary services, where the availability of a licensed band at a link is denoted by the probability. For instance, $q_{AB}^1 = 0.7$ for band 1 at link l_{AB} , $q_{BC}^1 = 0.6$ for band 1 at link l_{BC} and $q_{BC}^2 = 0.8$ for the band 2 at link l_{BC} as shown in Fig. 2a. Furthermore, we use $d(\cdot)$ to represent euclidean distance and suppose that $d(A, B) = d(B, C) = d(C, D) = d(D, E) = D_T = \frac{1}{2}D_I$, $d(A, C) = \sqrt{2}D_T$, $d(A, D) = \sqrt{5}D_T$, and $d(A, E) = \sqrt{10}D_T$, where D_T and D_I are the transmission range and interference range of the CR users, respectively.

Given the above assumptions and information about toy CRNs, we can construct the corresponding 4D conflict graph, which is depicted in Fig. 2b. In the figure, each vertex corresponds to an LBP² quadruplet, for example, vertex $(l_{AB}, 1, 0.7, 1)$ in the 4D conflict graph corresponds to LBP² quadruplet $(l_{AB}, 1, 0.7, 1)$. Note that there are edges

between vertices $(l_{AB}, 1, 0.7, 1)$ and $(l_{BC}, 1, 0.6, 1)$, and $(l_{AB}, 1, 0.7, 1)$ and $(l_{BC}, 2, 0.8, 2)$ because l_{AB} and l_{BC} have a CR node B in common. There are edges between vertices $(l_{AB}, 1, 0.7, 1)$ and $(l_{CD}, 1, 0.9, 3)$ because l_{AB} is incident to l_{CD} over band 1. Moreover, there is an edge between vertices $(l_{BC}, 1, 0.6, 1)$ and $(l_{BC}, 2, 0.8, 2)$ because any CR user has only one radio and can only work on one band at one time. Similar analysis applies to the other vertices in the 4D conflict graph as well.

4.2 Independent Sets and Conflict Cliques

Given a 4D conflict graph $\mathcal{G} = (\mathcal{V}, \mathcal{E})$ representing CRNs, we describe the impact of vertex $i \in \mathcal{V}$ on vertex $j \in \mathcal{V}$ as follows:

$$w_{ij} = \begin{cases} 1, & \text{if there is an edge connecting vertex } i \text{ and } j, \\ 0, & \text{if there is no edge between vertex } i \text{ and } j, \end{cases} \quad (1)$$

where the two vertices correspond to two LBP² quadruplets, respectively.

Provided that there is a vertex/LBP² quadruplet set $\mathcal{I} \subseteq \mathcal{V}$ and an LBP² quadruplet $i \in \mathcal{I}$ satisfying $\sum_{j \in \mathcal{I}, i \neq j} w_{ij} < 1$, the transmission at LBP² quadruplet i will be successful even if all the other LBP² quadruplets belonging to the set \mathcal{I} are transmitting at the same time. If any $i \in \mathcal{I}$ satisfies the condition above, we can schedule the transmissions over all these LBP² quadruplets in \mathcal{I} to be active simultaneously. Such a vertex/LBP² quadruplet set \mathcal{I} is called an independent set. If adding any one more LBP² quadruplet into an independent set \mathcal{I} results in a nonindependent one, \mathcal{I} is defined as a maximum independent set. Besides, if there exists a vertex/LBP² quadruplet set $\mathcal{Z} \subseteq \mathcal{V}$ in \mathcal{G} and any two LBP² quadruplets i and j in \mathcal{Z} satisfying $w_{ij} \neq 0$ (i.e., vertex i and j cannot be scheduled to transmit successfully at the same time.), \mathcal{Z} is called a conflict clique. If \mathcal{Z} is no longer a conflict clique after adding any one more LBP² quadruplet, \mathcal{Z} is defined as a maximum conflict clique.

5 OPTIMAL PATH SELECTION UNDER LINK SCHEDULING, ROUTING, AND BUDGET CONSTRAINTS

In this section, we study how the SSP can find the optimal path with the highest throughput under multiple constraints. First, we address how to calculate the path capacity considering link scheduling for a given path. Then, we mathematically describe flow routing constraints for single-radio-based CR users. After that, we formulate an integer linear programming optimization problem to find the best possible path to achieve the maximum end-to-end throughput under CR scheduling, routing, and budget constraints in multihop CRNs.

5.1 Path Capacity under CR Link Scheduling Constraints

For a given path \mathcal{P} , we can establish the 4D conflict graph $\mathcal{G}_{\mathcal{P}} = (\mathcal{V}_{\mathcal{P}}, \mathcal{E}_{\mathcal{P}})$ following the same approach illustrated in Section 4.1. Suppose we can list all independent sets as $\mathcal{I}_{\mathcal{P}} = \{\mathcal{I}_1, \mathcal{I}_2, \dots, \mathcal{I}_m, \dots, \mathcal{I}_M\}$, where M is $|\mathcal{I}_{\mathcal{P}}|$, and $\mathcal{I}_m \subseteq \mathcal{V}_{\mathcal{P}}$ for $1 \leq m \leq M$. Then, at any time, at most one independent set can be active to transmit packets for all

LBP² quadruplets in that set. Let $\lambda_m \geq 0$ denote the time share scheduled to independent set \mathcal{I}_m , and

$$\sum_{1 \leq m \leq M} \lambda_m \leq 1, \quad \lambda_m \geq 0 \quad (1 \leq m \leq M). \quad (2)$$

Let $r_{ij}^b(\mathcal{I}_m)$ be the data rate for CR link l_{ij} over band b , where $r_{ij}^b(\mathcal{I}_m) = 0$ if LBP² quadruplet $(l_{ij}, b, q_{ij}^b, p_{ij}^b) \notin \mathcal{I}_m$; otherwise, $r_{ij}^b(\mathcal{I}_m)$ is the channel rate⁵ for l_{ij} over band b . Therefore, by exploiting the independent set \mathcal{I}_m , the flow rate that l_{ij} can support over band b in the time share λ_m is $\lambda_m r_{ij}^b(\mathcal{I}_m) q_{ij}^b$, considering the possible returning of primary services in CRNs. Let s represent the flow rate of a given CR session. This CR session is feasible at link l_{ij} if there exists a schedule of the independent sets satisfying

$$s \leq s_{ij} = \sum_{m=1}^M \lambda_m \sum_{b=1}^{|\mathcal{B}_i \cap \mathcal{B}_j|} r_{ij}^b(\mathcal{I}_m) q_{ij}^b. \quad (3)$$

To maximize the end-to-end throughput of \mathcal{P} , we must consider the traffic traveling through all links along the given path from the CR source to the CR destination, i.e.,

$$C_{\mathcal{P}} = \max \min_{l_{ij} \in \mathcal{P}} s_{ij}. \quad (4)$$

Let s_e denote $\min_{l_{ij} \in \mathcal{P}} s_{ij}$, where e is the bottleneck CR link along \mathcal{P} for the end-to-end throughput. As introduced in Section 3.1, the time is divided into spectrum trading periods with the duration of τ . Each trading period is further partitioned into a set of time slots indexed by m ($1 \leq m \leq M$), so that the m th time slot has a length of $\lambda_m \tau$. In the m th time slot, all LBP² quadruplets in the set \mathcal{I}_m will be scheduled to transmit. The end-to-end throughput of \mathcal{P} is determined by the throughput of the bottleneck link, i.e., s_e . So, during each spectrum trading period of length τ , the path capacity of \mathcal{P} is

$$s_e = \frac{1}{\tau} \sum_{m=1}^M \lambda_m \tau \sum_{b=1}^{|\mathcal{B}_i \cap \mathcal{B}_j|} r_e^b(\mathcal{I}_m) q_e^b = \sum_{m=1}^M \lambda_m \sum_{b=1}^{|\mathcal{B}_i \cap \mathcal{B}_j|} r_e^b(\mathcal{I}_m) q_e^b, \quad (6)$$

where $r_e^b(\mathcal{I}_m)$ and q_e^b represent the data rate and spectrum availability for the bottleneck link e over band b , respectively.

5.2 Single-Radio-Based CR Routing Constraints

As for routing, the SSP will help the source CR node to find the available paths and employ a number of relay CR nodes to forward the data packets toward its destination CR node. Similar to the modeling in [36] and [43], we mathematically present the routing constraints as follows.

Let f_{ij} represent the flow rate of the CR session over link l_{ij} , where $i \in \mathcal{N}$ and $j \in \bigcup_{b \in \mathcal{B}_i} \mathcal{T}_i^b$. Here, \mathcal{T}_i^b is the set of CR nodes within CR node i 's transmission range, when

5. In this paper, we assume channel rate is determined by the received power and is equal to the maximum available rate satisfying the requirement of receiver sensitivity. As we know, in most of existing literature [27], [34], [36], the channel rate is approximated by the physical channel capacity obtained from Shannon-Hartley theorem, even though the capacity cannot be achieved. Moreover, the channel rate here can easily be substituted by the more practical effective data rate, which is defined in [26]. Note that all these approximations and substitutions will not affect the theoretical results as well as performance comparison in this work.

band $b \in \mathcal{B}_i$ is opportunistically used. To simplify the notation, let $\mathcal{T}_i = \bigcup_{b \in \mathcal{B}_i} \mathcal{T}_i^b$.

If CR node i is the source node of the CR session, i.e., $i = s_r$, then

$$\sum_{j \in \mathcal{T}_i} f_{ij} = s, \quad (6)$$

$$\sum_{j \in \mathcal{T}_i} f_{ji} = 0. \quad (7)$$

Due to the inherent single-radio constraint of CR devices, we focus on the unicast and single-path routing problem. Thus, we need to modify the routing constraint in (6) as follows:

$$\sum_{j \in \mathcal{T}_i} f_{ij} \delta_{ij} = s, \quad (8)$$

where $\delta_{ij} = 1$ indicates that l_{ij} may have a nonzero flow, i.e.,

$$\sum_{j \in \mathcal{T}_i} \delta_{ij} \leq 1, \quad \delta_{ij} \in \{0, 1\}. \quad (9)$$

If CR node i is an intermediate relay node for the CR session, i.e., $i \neq s_r$ and $i \neq d_t$, then

$$\sum_{j \in \mathcal{T}_i} f_{ij} \delta_{ij} = \sum_{j \in \mathcal{T}_i} f_{ji} \delta_{ji}. \quad (10)$$

If CR node i is the destination node of the CR session, i.e., $i = d_t$, then

$$\sum_{j \in \mathcal{T}_i} f_{ji} \delta_{ji} = s. \quad (11)$$

Note that if (7), (8), (9), and (10) are satisfied, it can be easily verified that (11) must be satisfied. As a result, it is sufficient to list only (7), (8), (9), and (10) as routing constraints in the problem formulation.

5.3 Optimal Path Selection under Multiple Constraints

If there is more than one route available for the data delivery from the source CR node to the destination CR node, the SSP will select the optimal path on behalf of the source CR node in terms of the end-to-end throughput. Since the SSP purchases available licensed bands and charges the source CR node for the CR session's opportunistic usage of these bands as mentioned in Section 3.1, the SSP must consider the budget of the source CR node besides the CR link scheduling and routing constraints. Thus, the SSP seeks for a feasible solution to trading the available frequency bands, assigning these bands to CR nodes, scheduling bands for transmission and reception, and routing the CR flow so that the end-to-end throughput of the CR session is maximized in multihop CRNs.

The optimal path selection problem under multiple constraints in multihop CRNs can be formulated as follows:

$$\begin{aligned} & \text{Maximize } s \\ & \text{s.t. : } \sum_{j \in \mathcal{T}_i} f_{ji} = 0 \quad (i = s_r), \end{aligned} \quad (12)$$

$$\sum_{j \in \mathcal{T}_i} f_{ij} \delta_{ij} = s \quad (i = s_r), \quad (13)$$

$$\sum_{j \in \mathcal{T}_i} f_{ij} \delta_{ij} = \sum_{j \in \mathcal{T}_i} f_{ji} \delta_{ji} \quad (i \in \mathcal{N} \setminus \{s_r, d_t\}), \quad (14)$$

$$\sum_{j \in \mathcal{T}_i} \delta_{ij} \leq 1, \quad \delta_{ij} \in \{0, 1\}, \quad (i \in \mathcal{N}), \quad (15)$$

$$0 \leq f_{ij} \leq \sum_{m=1}^{|\mathcal{I}|} \lambda_m \sum_{b=1}^{|\mathcal{B}_i \cap \mathcal{B}_j|} r_{ij}^b(\mathcal{I}_m) q_{ij}^b, \quad (16)$$

$$\begin{aligned} & (i \in \mathcal{N}, j \in \mathcal{T}_i, b \in \mathcal{B}_i \cap \mathcal{B}_j \text{ and } \mathcal{I}_m \in \mathcal{I}) \\ & \sum_{m=1}^{|\mathcal{I}|} \lambda_m \leq 1, \quad \lambda_m \geq 0, \end{aligned} \quad (17)$$

$$\sum_{m=1}^{|\mathcal{I}|} \lambda_m \sum_{(l_{ij}, b, q_{ij}^b, p_{ij}^b) \in \mathcal{I}_m} p_{ij}^b \leq E \quad (18)$$

$$(i \in \mathcal{N}, j \in \mathcal{T}_i, b \in \mathcal{B}_i \cap \mathcal{B}_j \text{ and } \mathcal{I}_m \in \mathcal{I}),$$

where p_{ij}^b is the price charged for l_{ij} 's usage of band b , if LBP² quadruplet $(l_{ij}, b, q_{ij}^b, p_{ij}^b) \in \mathcal{I}_m$. As mentioned in Section 3.1, E is the budget of the source CR node. Correspondingly, (18) means that the overall expense of spectrum purchasing should be within the budget of the source CR node. In addition, (12), (13), (14), and (15) specify that there is at most one outgoing link from each CR node with a nonzero flow, and that there is only one path selected by the SSP between the CR source and the CR destination. Equations (16) and (17) indicate that the flow rates over l_{ij} cannot exceed the capacity of this CR link, which is obtained from the CR link scheduling as illustrated in Section 5.1.

Note that \mathcal{I} includes all independent sets in CRNs. Given all independent sets⁶ in the network, we find that the formulated optimization is a mixed-integer linear programming problem since δ_{ij} only has binary values. It can near-optimally be solved in polynomial time by some typical algorithms (e.g., sequential fixing algorithm [35], [36], branch and bound [45], etc.) or softwares (e.g., CPLEX [46]), provided that all the independent sets along different paths can be found in $\mathcal{G}(\mathcal{V}, \mathcal{E})$.

6 A HEURISTIC PATH SELECTION ALGORITHM FOR HIGH END-TO-END THROUGHPUT

As we know, to find all independent sets in $\mathcal{G}(\mathcal{V}, \mathcal{E})$ is NP-hard [25], [26], [27], [29], [44]. Even though a candidate path is given, it is too complex for the SSP to find all the independent sets along the path, if the number of links of the path or the number of available licensed bands for selection in CRNs is large. Therefore, in this section, we propose a seven-step heuristic algorithm for path selection

6. That is a general assumption used in existing literature [25], [26], [27], [33], [44] for obtaining throughput bounds or performance comparison, where both link scheduling and flow routing are considered.

with the objective of maximizing the end-to-end throughput for a CR session. Instead of using independent sets, we classify the edges in the 4D conflict graph into two types, layer the graph by the number of licensed bands, and leverage conflict cliques to find the path with the highest end-to-end throughput for the CR session under budget constraints.

6.1 A Counterexample for the Maximum Clique Approach

In SR-SC networks, Chen et al. [25], and Zhai and Fang [26] leverage the maximum local cliques to approximately select the path with the highest throughput. Unfortunately, this approach cannot be applied in CRNs. We take a toy CR path shown in Fig. 2a as a counterexample. Suppose that the packet length is 1 and the transmission time of a packet over all LBP² quadruplets is the same, which is equal to T . According to the local clique approach, $C_P \leq \frac{1}{4T}$ since the maximum local clique contains four LBP² quadruplets as shown in Fig. 2b. However, if we only consider band 1 for CR nodes' usage regardless of primary services' activities, $C_P \leq \frac{1}{3T}$ since the maximum local clique contains three LBP² quadruplets. Intuitively, if we consider both bands 1 and 2 for CR nodes' opportunistic accessing, the throughput of the toy path should be further improved. The paradox above indicates that the maximum local clique-based algorithm is no longer suitable for path selection in CRNs.

6.2 The Proposed Algorithm for Path Selection in CRNs

The detailed procedure of the proposed heuristic algorithm for path selection in CRNs is presented as follows:

Step 1: Construction of the 4D conflict graph.

Given a candidate path \mathcal{P} , we first set up a corresponding 4D conflict graph $\mathcal{G}_P(\mathcal{V}_P, \mathcal{E}_P)$ as illustrated in Section 4.1.

Step 2: Decoupling the 4D conflict graph into layers.

With the established 4D conflict graph of the path, we further divide $\mathcal{G}_P(\mathcal{V}_P, \mathcal{E}_P)$ into different layers according to the number of bands, i.e., $|\mathcal{B}|$. To put it in another way, each layer represents a band, and the intercepted conflict graph on layer b describes the interference relationship among the CR links over band b , $b \in \mathcal{B}$.

For example, for a path from CR node A to node E as shown in Fig. 2a, we build up the corresponding 4D conflict graph and divide the graph into two layers because the total number of available bands in CRNs is 2.

Step 3: Differentiating two types of edges.

Then, we classify the edges on a layer of the 4D conflict graph into two categories. For layer b in \mathcal{G}_P , one kind of edges connect two different LBP² quadruplets who have one CR node in common, i.e., LBP² quadruplets on layer b satisfying Condition 1. We define these edges as *nonreducible edges*. The other kind of edges connect two different LBP² quadruplets who have co-band interference, i.e., LBP² quadruplets on layer b satisfying Condition 2. We define these edges as *reducible edges*.

For example, in Fig. 3, edges between LBP² quadruplets $(l_{AB}, 1, 0.7, 1)$ and $(l_{BC}, 1, 0.6, 1)$, between $(l_{BC}, 1, 0.6, 1)$ and $(l_{CD}, 1, 0.9, 3)$, and between $(l_{CD}, 1, 0.9, 3)$ and $(l_{DE}, 1, 0.7, 1)$ on layer 1 are nonreducible edges (denoted by solid lines) due to the single-radio constraint; correspondingly, edges

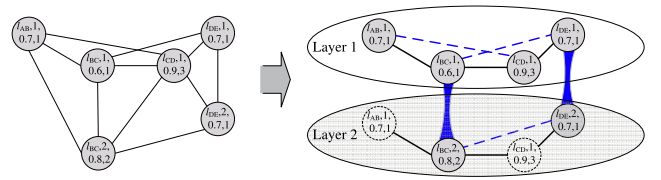


Fig. 3. An illustrative example for the proposed procedure with a given path.

between $(l_{AB}, 1, 0.7, 1)$ and $(l_{CD}, 1, 0.9, 3)$ and between $(l_{BC}, 1, 0.6, 1)$ and $(l_{DE}, 1, 0.7, 1)$ on layer 1, and edges between $(l_{BC}, 2, 0.8, 2)$ and $(l_{DE}, 2, 0.7, 1)$ on layer 2 are reducible edges (denoted by dashed lines). The co-band interference between LBP² quadruplets represented by reducible edges may be mitigated by switching LBP² quadruplets to different layers.

Step 4: Selecting the benchmark layer.

If there is only one layer in \mathcal{G}_P , select it as the benchmark layer; if there is more than one layer in \mathcal{G}_P , select the one which has the most edges (either nonreducible edges or reducible ones) because this layer can most effectively show the interference relationship among different links along the path \mathcal{P} . For instance, layer 1 is the benchmark layer for the toy CR path from CR node A to node E as shown in Fig. 3.

Step 5: Establishing the benchmark path capacity.

After choosing the benchmark layer, we further estimate the benchmark expense. To calculate the benchmark expense, we need information from two sides: 1) the unit price of the band used by a link and 2) the active time of that link along the path \mathcal{P} for one time period τ , under the condition that layer b of \mathcal{G}_P is selected as the benchmark layer.

Let l_{ij} be a CR link along the path \mathcal{P} , E_{ij} be the estimated expense of l_{ij} , and \mathcal{Q}_{ij} represent the LBP² quadruplet set associated with l_{ij} (e.g., $\mathcal{Q}_{DE} = \{(l_{DE}, 1, 0.7, 1), (l_{DE}, 2, 0.7, 1)\}$) as shown in Fig. 3). Given layer b as the benchmark layer, the unit price of the band used by l_{ij} is calculated as the following three cases:

- *Case 1:* If $|\mathcal{Q}_{ij}| = 1$, there is only one LBP² quadruplet available for l_{ij} . Thus, the SSP can only choose the LBP² quadruplet for l_{ij} and pay the corresponding price for using the band enclosed in that LBP² quadruplet.
- *Case 2:* If $|\mathcal{Q}_{ij}| \geq 1$ and $(l_{ij}, b, q_{ij}^b, p_{ij}^b) \in \mathcal{Q}_{ij}$, there are multiple LBP² quadruplets available for l_{ij} including $(l_{ij}, b, q_{ij}^b, p_{ij}^b)$. Since layer b is the benchmark layer, the SSP will choose LBP² quadruplet $(l_{ij}, b, q_{ij}^b, p_{ij}^b)$ for l_{ij} to calculate the benchmark expense and pay p_{ij}^b for using band b , i.e., $E_{ij} = p_{ij}^b$.
- *Case 3:* If $|\mathcal{Q}_{ij}| \geq 1$ and $(l_{ij}, b, q_{ij}^b, p_{ij}^b) \notin \mathcal{Q}_{ij}$, there are some other LBP² quadruplets available for l_{ij} except $(l_{ij}, b, q_{ij}^b, p_{ij}^b)$. In this case, the SSP can randomly choose an LBP² quadruplet $(l_{ij}, k, q_{ij}^k, p_{ij}^k)$ in \mathcal{Q}_{ij} for l_{ij} to estimate the benchmark expense and pay the corresponding price for using the band enclosed in that LBP² quadruplet, i.e., $E_{ij} = p_{ij}^k (k \neq b)$.

Then, we employ conflict cliques over layer b to estimate the active time of links along the path \mathcal{P} for one time period

τ . Similar to the illustration in [25] and [26], we define the interference clique transmission time $T_{\mathcal{Z}}$ for one conflict clique \mathcal{Z} over the selected benchmark layer as

$$T_{\mathcal{Z}} = \sum_{(l_{ij}, b, q_{ij}^b, p_{ij}^b) \in \mathcal{Z}} T_{(l_{ij}, b, q_{ij}^b, p_{ij}^b)}, \quad (19)$$

where $T_{(l_{ij}, b, q_{ij}^b, p_{ij}^b)}$ is the transmission time for a packet over l_{ij} using band b . Assume the packet length is 1, considering the activities of primary services, $T_{(l_{ij}, b, q_{ij}^b, p_{ij}^b)}$ can be written as

$$T_{(l_{ij}, b, q_{ij}^b, p_{ij}^b)} = \frac{1}{r_{ij}^b \cdot q_{ij}^b}, \quad (20)$$

For the given path \mathcal{P} , find the set \mathcal{Z} of all the maximum interference cliques \mathcal{Z} for the LBP² quadruplets on the benchmark layer. Let $T_{\mathcal{P}}$ be the maximum value of $T_{\mathcal{Z}}$ for all cliques over the benchmark layer and

$$T_{\mathcal{P}} = \max_{\mathcal{Z} \in \mathcal{Z}} T_{\mathcal{Z}}. \quad (21)$$

Considering the link l_{ij} in \mathcal{Z} and any one packet successfully delivered from the CR source to the CR destination, the packet takes time $T_{\mathcal{P}}$ to travel through all the LBP² quadruplets in \mathcal{Z} , and l_{ij} cannot be scheduled to do any other transmission during $T_{\mathcal{P}}$. That indicates that a packet takes at least time $T_{\mathcal{P}}$ at link l_{ij} over the benchmark layer, and the throughput at link l_{ij} is less than or equal to $\frac{1}{T_{\mathcal{P}}}$ over the benchmark layer. Since the end-to-end throughput cannot be larger than the throughput of any link along the path, the benchmark path capacity $C_{\mathcal{P}}$ can be approximated as $\frac{1}{T_{\mathcal{P}}}$ [26].

This statement holds if there are no odd cycles [47] in $\mathcal{G}_{\mathcal{P}}$. In fact, the problem can be simplified for the conflict graph constructed from general paths without odd cycles as illustrated in [26]. Instead of finding all the maximum cliques including one LBP² quadruplet, the SSP only needs to consider other LBP² quadruplets close to this one along the path. We refer to these cliques as the *local interference cliques* of a path. For paths over a certain layer, the maximum value of the interference clique transmission time of all local cliques (i.e., $\hat{T}_{\mathcal{P}}$ over benchmark layer) is equal to that for all cliques (i.e., $T_{\mathcal{P}}$ over benchmark layer).⁷

Thus, we can further establish the benchmark path capacity⁸ using $\hat{T}_{\mathcal{P}}$ as $C_{\mathcal{P}} = \frac{1}{\hat{T}_{\mathcal{P}}} = \frac{1}{T_{\mathcal{P}}}$ [26].

Step 6: Establishing the benchmark expense.

Given the benchmark path capacity $C_{\mathcal{P}}$, the SSP will establish the benchmark expense $\Pi_{\mathcal{P}}$.

For a CR link l_{ij} along the path \mathcal{P} , if the LBP² quadruplet $(l_{ij}, b, q_{ij}^b, p_{ij}^b) \in \mathcal{Q}_{ij}$, i.e., the LBP² quadruplet $(l_{ij}, b, q_{ij}^b, p_{ij}^b)$ is on the benchmark layer b , it takes up t_{ij} for packet delivery during one period τ , where t_{ij} is

$$t_{ij} = \frac{\tau C_{\mathcal{P}}}{r_{ij}^b q_{ij}^b} = \frac{\tau T_{(l_{ij}, b, q_{ij}^b, p_{ij}^b)}}{\hat{T}_{\mathcal{P}}}. \quad (22)$$

7. Some brute-force algorithms can be designed to find all local cliques on a specific layer (i.e., for a specific band) in polynomial time as illustrated in [26], which is omitted in this paper due to the limited space.

8. Similar to [25] and [26], in this paper, we only consider the direct routes as defined in [26]. Note that for direct routes, $C_{\mathcal{P}} = \frac{1}{T_{\mathcal{P}}} = \frac{1}{\hat{T}_{\mathcal{P}}}$ holds.

Correspondingly, the benchmark expense of l_{ij} is

$$\Pi_{ij} = \frac{E_{ij} \tau T_{(l_{ij}, b, q_{ij}^b, p_{ij}^b)}}{\tau \hat{T}_{\mathcal{P}}} = \frac{E_{ij} T_{(l_{ij}, b, q_{ij}^b, p_{ij}^b)}}{\hat{T}_{\mathcal{P}}}. \quad (23)$$

Similarly, for a CR link l_{uw} along the path, where the LBP² quadruplet $(l_{uw}, b, q_{uw}^b, p_{uw}^b) \notin \mathcal{Q}_{uw}$ and band k other than band b is exploited by l_{uw} for packet delivery, the benchmark expense is written as

$$\Pi_{uw} = \frac{E_{uw} T_{(l_{uw}, k, q_{uw}^k, p_{uw}^k)}}{\hat{T}_{\mathcal{P}}}. \quad (24)$$

Therefore, the benchmark expense of the path \mathcal{P} can be expressed as

$$\begin{aligned} \Pi_{\mathcal{P}} = & \sum_{(l_{ij}, b, q_{ij}^b, p_{ij}^b) \in \mathcal{Q}_{ij}} \frac{T_{(l_{ij}, b, q_{ij}^b, p_{ij}^b)}}{\hat{T}_{\mathcal{P}}} E_{ij} \\ & + \sum_{(l_{uw}, b, q_{uw}^b, p_{uw}^b) \notin \mathcal{Q}_{uw}} \frac{T_{(l_{uw}, k, q_{uw}^k, p_{uw}^k)}}{\hat{T}_{\mathcal{P}}} E_{uw}. \end{aligned} \quad (25)$$

The procedure of Steps 5 and 6 is summarized in Algorithm 1.

Algorithm 1. Establishing the benchmark expense

Require: Initialize the procedure after layering $\mathcal{G}_{\mathcal{P}}$ and selecting layer b as the benchmark layer.

- 1: **for all** $l_{ij} \in \mathcal{P}$ **do**
- 2: **if** $|\mathcal{Q}_{ij}| == 1$ **then**
- 3: The SSP chooses that LBP² quadruplet for l_{ij} .
- 4: **else if** $|\mathcal{Q}_{ij}| \geq 1$ and $(l_{ij}, b, q_{ij}^b, p_{ij}^b) \in \mathcal{Q}_{ij}$ **then**
- 5: The SSP chooses $(l_{ij}, b, q_{ij}^b, p_{ij}^b)$ for l_{ij} and set $E_{ij} = p_{ij}^b$.
- 6: **else if** $|\mathcal{Q}_{ij}| \geq 1$ and $(l_{ij}, b, q_{ij}^b, p_{ij}^b) \notin \mathcal{Q}_{ij}$ **then**
- 7: The SSP randomly chooses $(l_{ij}, k, q_{ij}^k, p_{ij}^k) \in \mathcal{Q}_{ij}$ for l_{ij} and set $E_{ij} = p_{ij}^k$.
- 8: **end if**
- 9: Calculate the transmission time for $l_{ij} \in \mathcal{P}$.
- 10: **end for**
- 11: Find the maximum value of the local clique's transmission time $\hat{T}_{\mathcal{P}}$ and estimate the benchmark path capacity with $\frac{1}{\hat{T}_{\mathcal{P}}}$.
- 12: Given the benchmark path capacity, calculate the transmission time and the corresponding benchmark expense at $l_{ij} \in \mathcal{P}$.
- 13: Sum up the benchmark expense of each link along \mathcal{P} and establish the benchmark expense of \mathcal{P} .

Step 7: Switching quadruplets for high throughput.

Depending on the values of $\Pi_{\mathcal{P}}$, $\frac{1}{\hat{T}_{\mathcal{P}}}$, and the budget E , the SSP may apply different strategies to switch LBP² quadruplets.

If $\Pi_{\mathcal{P}}$ is beyond E , i.e., the budget of the CR source, the SSP will switch LBP² quadruplets to reduce the overall expense for the given path \mathcal{P} . Note that $\Pi_{\mathcal{P}}$ increases when $\hat{T}_{\mathcal{P}}$ decreases as shown in (25). Thus, the SSP would switch the LBP² quadruplets on other layers (i.e., $(l_{uw}, k, q_{uw}^k, p_{uw}^k)$ in (25), where $(l_{uw}, b, q_{uw}^b, p_{uw}^b) \notin \mathcal{Q}_{uw}$) rather than the ones on the benchmark layer (i.e., $(l_{ij}, b, q_{ij}^b, p_{ij}^b)$ in (25), where $(l_{ij}, b, q_{ij}^b, p_{ij}^b) \in \mathcal{Q}_{ij}$) to lower down the expense. The SSP

will replace $(l_{uv}, k, q_{uv}^k, p_{uv}^k)$ with $(l_{uv}, h, q_{uv}^h, p_{uv}^h)$, where $p_{uv}^h < p_{uv}^k$ and $(l_{uv}, h, q_{uv}^h, p_{uv}^h) \in \mathcal{Q}_{uv}$. By switching LBP² quadruplets, if the overall expense of \mathcal{P} can be reduced to the budget of CR source, the path capacity of \mathcal{P} , i.e., $C_{\mathcal{P}}^*$ can be estimated with the benchmark path capacity, i.e., $C_{\mathcal{P}} = \frac{1}{T_{\mathcal{P}}}$. Otherwise, path \mathcal{P} is not feasible for the CR session due to budget constraints.

On the other hand, if $\Pi_{\mathcal{P}}$ is below E , the SSP will switch LBP² quadruplets to improve the throughput of the path \mathcal{P} .

From (19) and (21), and $C_{\mathcal{P}} = \frac{1}{T_{\mathcal{P}}} = \frac{1}{T_{\mathcal{P}}}$, we find that if the number of LBP² quadruplets in the conflict clique can be reduced, the throughput of the path will increase. Moreover, it is obvious that the co-band interference between LBP² quadruplets, which are the vertices of *reducible edges* defined in Step 3, can be mitigated by switching LBP² quadruplets. Therefore, the SSP will switching LBP² quadruplets to increase the path capacity under the budget E as follows.

The SSP first sorts the LBP² quadruplets on the benchmark layer. According to the number of *reducible edges* associated with the LBP² quadruplets, the SSP indexes the LBP² quadruplets in a decreasing manner, i.e., the more *reducible edges* an LBP² quadruplet is associated with, the smaller index number the LBP² quadruplet has.⁹

Then, the SSP starts the switching process with the LBP² quadruplet having the smallest index. Let the LBP² quadruplet be $(l_{ij}, b, q_{ij}^b, p_{ij}^b)$ on benchmark layer b . If $|\mathcal{Q}_{ij}| = 1$, then this LBP² quadruplet cannot be switched, and the SSP continues to check the next LBP² quadruplet. Otherwise, if $|\mathcal{Q}_{ij}| > 1$, the SSP needs to decide whether $(l_{ij}, b, q_{ij}^b, p_{ij}^b)$ can be switched into $(l_{ij}, k, q_{ij}^k, p_{ij}^k)$, where $(l_{ij}, k, q_{ij}^k, p_{ij}^k) \in \mathcal{Q}_{ij}$ and $k \neq b$. Let $\hat{T}_{\mathcal{P}}$ be the transmission time of local cliques on the benchmark layer b before quadruplet switching, $\hat{T}'_{\mathcal{P}}$ be the largest transmission time of local cliques among all the layers after switching $(l_{ij}, b, q_{ij}^b, p_{ij}^b)$ to $(l_{ij}, k, q_{ij}^k, p_{ij}^k)$, and $\Pi'_{\mathcal{P}}$ be the expense of \mathcal{P} after switching $(l_{ij}, b, q_{ij}^b, p_{ij}^b)$ to $(l_{ij}, k, q_{ij}^k, p_{ij}^k)$. To make the decision of quadruplet switching, the SSP must consider the following two cases:

- If $\hat{T}'_{\mathcal{P}} \leq \hat{T}_{\mathcal{P}}$ and $\Pi'_{\mathcal{P}} \leq E$, the SSP will switch $(l_{ij}, b, q_{ij}^b, p_{ij}^b)$ to $(l_{ij}, k, q_{ij}^k, p_{ij}^k)$, eliminate *reducible edges* associated with LBP² quadruplet $(l_{ij}, b, q_{ij}^b, p_{ij}^b)$ on layer b , and add *reducible edges* associated with LBP² quadruplet $(l_{ij}, k, q_{ij}^k, p_{ij}^k)$ on layer k . In addition, the SSP will identify the layer with $\hat{T}'_{\mathcal{P}}$, put $\hat{T}_{\mathcal{P}} = \hat{T}'_{\mathcal{P}}$ and $\Pi_{\mathcal{P}} = \Pi'_{\mathcal{P}}$, and set that layer as new benchmark layer. After that, the SSP will sort LBP² quadruplets on the new benchmark layer and continue switching process.
- If $\hat{T}'_{\mathcal{P}} > \hat{T}_{\mathcal{P}}$ or $\Pi'_{\mathcal{P}} > E$, the SSP cannot switch $(l_{ij}, b, q_{ij}^b, p_{ij}^b)$ to $(l_{ij}, k, q_{ij}^k, p_{ij}^k)$. The SSP will keep the benchmark layer and benchmark expense unchanged, and continue the process with the next LBP² quadruplet.

9. If there are multiple LBP² quadruplets with the same number of *reducible edges*, the SSP will just index them in order according to their distance from the CR source.

Iterations of quadruplet switching continue until $\hat{T}_{\mathcal{P}}$ cannot be decreased further under the CR source's budget E . Then, the SSP can estimate the throughput of \mathcal{P} as $C_{\mathcal{P}}^* = \frac{1}{\hat{T}_{\mathcal{P}}}$ as shown in Algorithm 2.

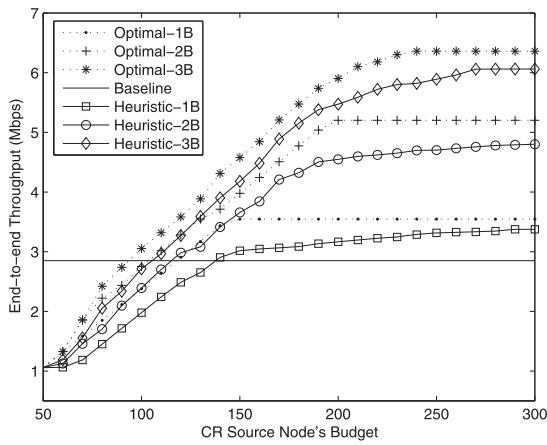
Algorithm 2. Switching quadruplets for high throughput
Require:The benchmark layer is layer b and $\Pi_{\mathcal{P}} \leq E$.

- 1: Sort and index the LBP² quadruplets on the benchmark layer in a decreasing manner according to the number of *reducible edges* associated with these quadruplets.
- 2: Set $\alpha = 1$.
- 3: Start the switching-quadruplet process of the α th quadruplet $(l_{ij}, b, q_{ij}^b, p_{ij}^b)$ on the benchmark layer.
- 4: **if** $|\mathcal{Q}_{ij}| == 1$ **then**
- 5: $\alpha = \alpha + 1$. Go to *Line 2*.
- 6: **else if** $|\mathcal{Q}_{ij}| \geq 1$ **then**
- 7: **for all** $(l_{ij}, k, q_{ij}^k, p_{ij}^k) \in \mathcal{Q}_{ij}$ **do**
- 8: Calculate $\hat{T}'_{\mathcal{P}}$ and $\Pi'_{\mathcal{P}}$
- 9: **if** $\hat{T}'_{\mathcal{P}} > \hat{T}_{\mathcal{P}}$ or $\Pi'_{\mathcal{P}} > E$ **then**
- 10: **continue**.
- 11: **else if** $\hat{T}'_{\mathcal{P}} \leq \hat{T}_{\mathcal{P}}$ and $\Pi'_{\mathcal{P}} \leq E$ **then**
- 12: Switch $(l_{ij}, b, q_{ij}^b, p_{ij}^b)$ into $(l_{ij}, k, q_{ij}^k, p_{ij}^k)$.
- 13: Delete the *reducible edges* associated with $(l_{ij}, b, q_{ij}^b, p_{ij}^b)$ on the benchmark layer.
- 14: Identify the layer with $\hat{T}'_{\mathcal{P}}$, and set that layer as new benchmark layer.
- 15: $\hat{T}_{\mathcal{P}} = \hat{T}'_{\mathcal{P}}$ and $\Pi_{\mathcal{P}} = \Pi'_{\mathcal{P}}$. Go to *Line 2*.
- 16: **end if**
- 17: **end for**
- 18: $\alpha = \alpha + 1$. Go to *Line 2*.
- 19: **end if**
- 20: Output the throughput of \mathcal{P} : $C_{\mathcal{P}}^* = \frac{1}{\hat{T}_{\mathcal{P}}} = \frac{1}{T_{\mathcal{P}}}$.

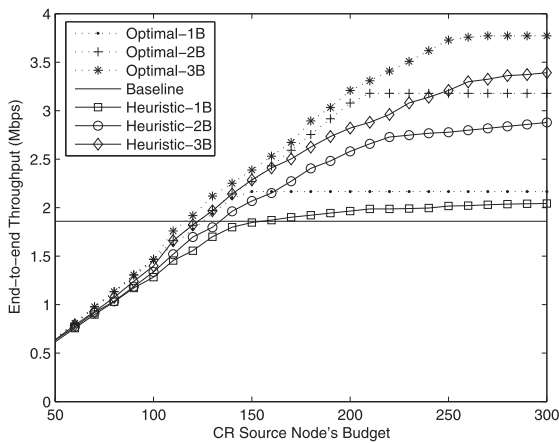
The heuristic algorithm provides a useful metric to the SSP for the path selection. Given possible paths of a CR session, the SSP can exploit the proposed algorithm above to calculate the throughput of these paths by using local cliques, and select the path with the highest path capacity.

6.3 Complexity Analysis

For a $\mathcal{G}_{\mathcal{P}}(\mathcal{V}_{\mathcal{P}}, \mathcal{E}_{\mathcal{P}})$ constructed from the candidate path \mathcal{P} , it is NP-hard to identify all the maximum independent sets. Given all the maximum independent sets and relaxed δ_{ij} -variables, the complexity of solving such an optimization problem by standard solvers such as CPLEX [46] is $\mathcal{O}(X^3Y)$ [45], where X is the number of variables and Y is the number of bits required to store the data. By contrast, the proposed heuristic algorithm can directly calculate the path capacity in each iteration. Thus, the complexity of the proposed algorithm mainly lies in the number of required iterations. Note that for a given candidate path, in each iteration, we determine the status of an additional link on an available band for the session under budget constraints. Let $|\mathcal{N}_{\mathcal{P}}|$ be the number of CR nodes along the path, and $|\mathcal{H}| = \max_{i \in \mathcal{N}_{\mathcal{P}}, b \in \mathcal{B}_i} |\mathcal{H}_i^b|$, where $|\mathcal{H}_i^b|$ is the number of CR nodes within the local clique of i over band b . Each link could be active at most $|\mathcal{B}|$ bands. So, for a path with $|\mathcal{N}_{\mathcal{P}}|$ CR nodes, the number of iterations for the proposed procedure is no more than the product $|\mathcal{N}_{\mathcal{P}}|^2 \cdot |\mathcal{H}| \cdot |\mathcal{B}|$, which indicates that the proposed algorithm has a polynomial-time complexity.



(a) Performance comparison among different path selection algorithms, where channel rate is 18M.



(b) Performance comparison among different path selection algorithms, where channel rate is 11M.

Fig. 4. Impact of CR source's budget on path selection in multihop CRNs.

7 PERFORMANCE EVALUATION

7.1 Simulation Setup

We consider a multihop CRN consisting of $|\mathcal{N}| = 40$ CR nodes randomly distributed in a $800 * 800 \text{ m}^2$ area. We assume each CR node has a fixed transmission range of 250 m and interference range of 500 m [44], [48]. Regarding the returning of primary services, the availability of a licensed band over a CR link at a certain location is with a random probability within $(0.5, 1]$, i.e., $q_{i,j}^b \in (0.5, 1]$ ($\forall i, j \in \mathcal{N}$ and $\forall b \in \mathcal{B}$). Correspondingly, the price for opportunistic using a band for one time period is within $(50, 100]$. The price of a licensed band increases with the availability of that band, given the fact that all bands have the identical bandwidth. For illustrative purposes, we conduct simulations to study the path selection problem in CRNs with two different channel rates, i.e., 18 Mbps (802.11a) and 11 Mbps (802.11b), respectively.

We fix the CR node nearest to the upper left corner as the CR source and the CR node nearest to the lower right corner as the CR destination. We compare the path selection algorithms consisting of the optimal path selection, the proposed heuristic path selection and the single-band-based

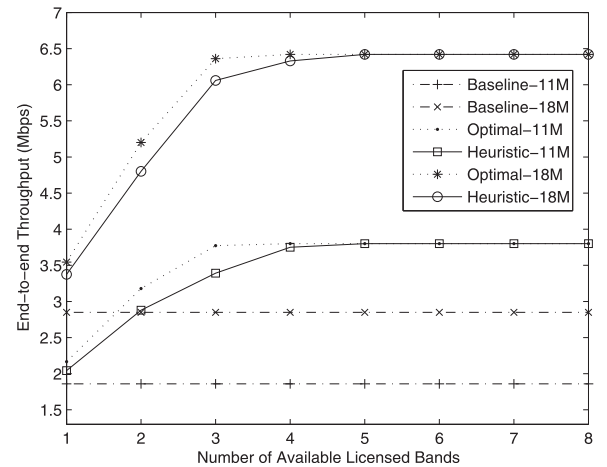


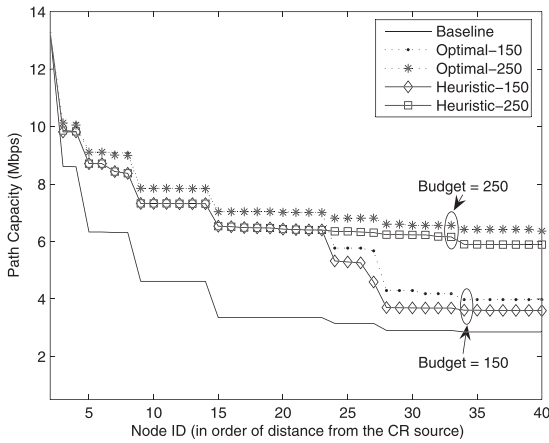
Fig. 5. Impact of the number of available licensed bands on path selection in multihop CRNs.

path selection illustrated in [26]. The performance metric is the end-to-end throughput/path capacity. Note that the optimal path selection is the one obtained from the mixed integer-linear programming problem formulated in Section 5.3. Given such a small network topology in simulations, we can find the independent sets [26], [27], relax the binary requirement on δ_{ij} and solve the optimization problem in a reasonable time by using CPLEX [46]. Besides, we demonstrate the impact of CR source's budget and the impact of the number of available licensed bands on the path capacity in CRNs, and present the results in Figs. 4 and 5. We also find the paths from the CR source to all the other CR nodes in this area, carry out simulations to evaluate the impact of distance from the CR source on the path capacity with different path selection algorithms, and show the results in Fig. 6.

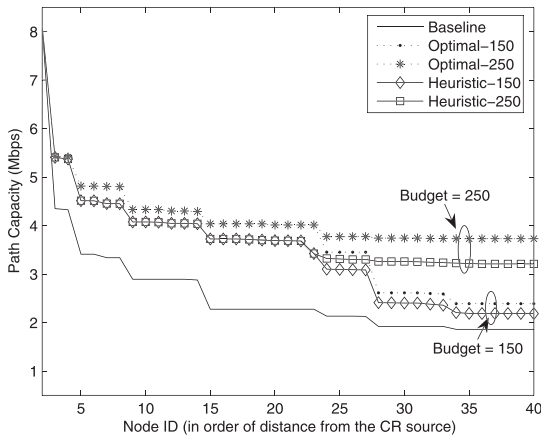
7.2 Results and Analysis

In Fig. 4, we compare the optimal path selection with the proposed heuristic path selection at different CR source's budget levels, where the number of available licensed bands $|\mathcal{B}|$ is equal to 1, 2, and 3, respectively. Meanwhile, we set the path capacity obtained from the single-band-based path selection algorithm in [26] as the baseline, where we assume the budget is large enough. From the results shown in Figs. 4a and 4b, four observations can be made in order. First, the single-band-based path selection has the worst performance among all these algorithms. That is not surprising because the single-band-based path selection algorithm in [26] is designed for SR-SC networks. It neither considers the CR capability of the CR relay nodes nor considers the possible returning of primary services at different CR links¹⁰ in CRNs. Second, as the number of available bands increases, the end-to-end throughput increases as well. The reason is that more licensed bands available give more opportunities for CR users' accessing, so that more CR links along the selected path can be activated for transmission simultaneously. Third, as the CR source's budget increases, the end-to-end throughput also increases. That is because the budget is one of the most

10. In the simulations, we assume there exist perfect links, where the delivery ratio is equal to 1. The packet loss of CR transmissions is only caused by the returning of primary services.



(a) Performance comparison among different path selection algorithms, where channel rate is 18M.



(b) Performance comparison among different path selection algorithms, where channel rate is 11M.

Fig. 6. Path capacity for different path selection algorithms in CRNs.

important concerns of the SSP when it jointly conducts the flow routing and link scheduling for a CR session. However, when the budget of CR source node is large enough (e.g., beyond 250), it has no impact on the SSP’s decision of path selection and the path capacity will not increase any more. Fourth, the performance of the heuristic algorithm is close to that of the optimal one at different budget levels as shown in Figs. 4a and 4b.

Fig. 5 presents the impact of the number of available bands on the path capacity in CRNs, where we can have the following two observations. 1) The path capacity obtained from the heuristic path selection algorithm is close to that from the optimal one, especially when the number of available licensed bands is larger than 4. 2) The increment of path capacity basically stops when the number of available bands exceeds 4. As illustrated in Sections 4.1 and 6, only the interference between LBP² quadruplets satisfying *Condition 2* can be reduced by switching LBP² quadruplets, due to the single-radio constraint of CR devices. Given the network scale in the simulation, there are a limited number of LBP² quadruplets satisfying *Condition 2* in the maximal conflict cliques. Therefore, the maximum path capacity can be achieved by full exploitation of four licensed bands, even

considering the potential interruption caused by primary services in multihop CRNs.

Fig. 6 shows the impact of distance between the CR source and destination on the path capacity in CRNs. For the simplicity of computing independent sets [27], we assume there are three licensed bands available in the network. Except for the observations we already have in Figs. 4 and 5, we find that the longer distance the path spans, the more likely the path capacity is affected by the budget of the CR source. It is obvious that a longer path may include more CR links along the path, which implies that more links could be scheduled to transmit at the same time. Thus, the end-to-end throughput of such a path depends more on the budget of the CR source.

8 CONCLUSION AND FUTURE WORK

In this paper, we have studied the path selection problem in multihop CRNs under flow routing, link scheduling and CR source’s budget constraints. We first introduce a novel service provider for CR users, SSP, and make the SSP help a given CR session to purchase the licensed spectrum and select the path for packet delivery. Then, considering the inherent single-radio constraint of CR devices and the features of spectrum trading, we propose a 4D conflict graph to describe the conflict relations among CR links. After that, we mathematically formulate the path selection problem under multiple constraints into an optimization problem with the objective of maximizing the end-to-end throughput for the CR session. Given all independent sets in 4D conflict graph, we can relax the formulated optimization problem and solve it by linear programming. Regarding the NP-hardness of finding all independent sets, we provide a heuristic algorithm as well, which layers the 4D conflict graph and exploits the maximum local cliques to approximately select the path with the highest throughput. By simulations, we demonstrate how the CR source’s budget, the number of available bands and distance from CR source affect the performance of path selection in terms of path capacity. We also compare the heuristic path selection algorithm with the optimal one and show that the throughput obtained from the heuristic algorithm is close to that obtained from the optimal one in multihop CRNs.

As an initial step, in this work, we just consider a single-flow scenario and ignore the interference from the other flows as well as the competitive bidding for spectrum usage from the other flows. In a CRN with multiflows, the CR source nodes need to develop sophisticated bidding strategies considering the competition from the peer flows, and the SSP should jointly consider the cross-layer factors and the bidding values to determine the sharing of the harvested spectrum. Besides, the network performance improvement is still hindered by the inherent single-radio of CR devices. Another issue is the mobility of CR users, which may have negative impact on the scheduled transmissions. Similar to multihop cellular networks, a better CRN architecture involving some fixed multiradio CR routers may further increase the network capacity and solve the mobility problem. The more complex design of path selection algorithms associated with multiflows in mobile CRNs will be deferred for our future research.

ACKNOWLEDGMENTS

This work was partially supported by the US National Science Foundation (NSF) under grant ECCS-1129062. The work of M. Pan was also partially supported by the NSF under grant NSF-1137732. The work of C. Zhang was partially supported by National Natural Science Foundation of China under Grant 61202140.

REFERENCES

- [1] Federal Communication Commission, "Spectrum Policy Task Force Report," ET Docket Nos. 02-135, Nov. 2002.
- [2] J. Mitola, "Cognitive Radio: An Integrated Agent Architecture for Software Defined Radio," PhD thesis, Royal Inst. of Technology, May 2000.
- [3] I. Akyildiz, W. Lee, M. Vuran, and M. Shantidev, "Next Generation/Dynamic Spectrum Access/Cognitive Radio Wireless Networks: A Survey," *Computer Networks J.*, vol. 50, no. 4, pp. 2127-2159, Sept. 2006.
- [4] D. Chen, S. Yin, Q. Zhang, M. Liu, and S. Li, "Mining Spectrum Usage Data: A Large-Scale Spectrum Measurement Study," *Proc. ACM MobiCom*, Sept. 2009.
- [5] S.M. Mishra, D. Cabric, C. Chang, D. Willkomm, B.V. Schewick, A. Wolisz, and R.W. Brodersen, "A Real Time Cognitive Radio Testbed for Physical and Link Layer Experiments," *Proc. IEEE Int'l Symp. New Frontiers in Dynamic Spectrum Access Networks (DySPAN '05)*, Nov. 2005.
- [6] M. McHenry, "Spectrum White Space Measurements," New American Foundation Broadband Forum, June 2003.
- [7] M.A. McHenry, P.A. Tenhula, D. McCloskey, D.A. Roberson, and C.S. Hood, "Chicago Spectrum Occupancy Measurements and Analysis and a Long-Term Studies Proposal," *Proc. First Int'l Workshop Technology and Policy for Accessing Spectrum (TAPAS)*, Aug. 2006.
- [8] D. Grandblaise, P. Bag, P. Levine, K. Moessner, and M. Pan, "Microeconomics Inspired Mechanisms to Manage Dynamic Spectrum Allocation," *Proc. IEEE Int'l Symp. New Frontiers in Dynamic Spectrum Access Networks (DySPAN '07)*, Apr. 2007.
- [9] S. Sengupta and M. Chatterjee, "An Economic Framework for Dynamic Spectrum Access and Service Pricing," *IEEE/ACM Trans. Networking*, vol. 17, no. 4, pp. 1200-1213, Aug. 2009.
- [10] B. Wang, Z. Han, and K.J.R. Liu, "Distributed Relay Selection and Power Control for Multiuser Cooperative Communication Networks Using Buyer/Seller Game," *Proc. IEEE INFOCOM*, May 2007.
- [11] B. Wang, Z. Ji, and K.J.R. Liu, "Primary-Prioritized Markov Approach for Dynamic Spectrum Access," *Proc. IEEE Int'l Symp. New Frontiers in Dynamic Spectrum Access Networks (DySPAN '07)*, Apr. 2007.
- [12] M. Pan, F. Chen, X. Yin, and Y. Fang, "Fair Profit Allocation in the Spectrum Auction Using the Shapley Value," *Proc. IEEE Global Telecomm. Conf. (GlobeCom '09)*, Dec. 2009.
- [13] J. Zhang and Q. Zhang, "Stackelberg Game for Utility-Based Cooperative Cognitive Radio Networks," *Proc. ACM MobiHoc*, May 2009.
- [14] X. Zhou, S. Gandhi, S. Suri, and H. Zheng, "eBay in the Sky: Strategy-Proof Wireless Spectrum Auctions," *Proc. ACM MobiCom*, Sept. 2008.
- [15] X. Zhou and H. Zheng, "Trust: A General Framework for Truthful Double Spectrum Auctions," *Proc. IEEE INFOCOM*, Apr. 2009.
- [16] J. Jia, Q. Zhang, Q. Zhang, and M. Liu, "Revenue Generation for Truthful Spectrum Auction in Dynamic Spectrum Access," *Proc. ACM MobiHoc*, May 2009.
- [17] Y. Wu, B. Wang, K.J. Liu, and T. Clancy, "A Multi-Winner Cognitive Spectrum Auction Framework with Collusion-Resistant Mechanisms," *Proc. IEEE Int'l Symp. New Frontiers in Dynamic Spectrum Access Networks (DySPAN '08)*, Oct. 2008.
- [18] Y. Xing, R. Chandramouli, and C. Cordeiro, "Price Dynamics in Competitive Agile Spectrum Access Markets," *IEEE J. Selected Areas in Comm.*, vol. 25, no. 3, pp. 613-621, Apr. 2007.
- [19] D. Niyato and E. Hossain, "Competitive Pricing for Spectrum Sharing in Cognitive Radio Networks: Dynamic Game, Inefficiency of Nash Equilibrium, and Collusion," *IEEE J. Selected Areas in Comm.*, vol. 26, no. 1, pp. 192-202, Jan. 2008.
- [20] D. Niyato, E. Hossain, and Z. Han, "Dynamics of Multiple-Seller and Multiple-Buyer Spectrum Trading in Cognitive Radio Networks: A Game Theoretic Modeling Approach," *IEEE Trans. Mobile Computing*, vol. 8, no. 8, pp. 1009-1022, Aug. 2009.
- [21] M. Pan, C. Zhang, P. Li, and Y. Fang, "Spectrum Harvesting and Sharing in Multi-Hop CRNs Under Uncertain Spectrum Supply," *IEEE J. Selected Areas in Comm.*, vol. 30, no. 2, pp. 369-378, Feb. 2012.
- [22] M. Pan, H. Yue, Y. Fang, and H. Li, "The X Loss: Band-Mix Selection for Opportunistic Spectrum Accessing with Uncertain Spectrum Supply From Primary Service Providers," *IEEE Trans. Mobile Computing*, vol. 11, no. 12, pp. 2133-2144, Dec. 2012.
- [23] M. Pan, H. Yue, Y. Fang, and H. Li, "The X Loss: Band-Mix Selection with Uncertain Supply for Opportunistic Spectrum Accessing," *Proc. IEEE Global Telecomm. Conf. (GlobeCom '09)*, Dec. 2010.
- [24] M. Pan, Y. Song, P. Li, and Y. Fang, "Reward and Risk for Opportunistic Spectrum Accessing in Cognitive Radio Networks," *Proc. IEEE Global Telecomm. Conf. (GlobeCom '09)*, Dec. 2010.
- [25] F. Chen, H. Zhai, and Y. Fang, "Available Bandwidth in Multirate and Multihop Wireless Ad Hoc Networks," *IEEE J. Selected Areas in Comm.*, vol. 28, no. 3, pp. 299-307, Apr. 2010.
- [26] H. Zhai and Y. Fang, "Impact of Routing Metrics on Path Capacity in Multirate and Multihop Wireless Ad Hoc Networks," *Proc. IEEE Int'l Conf. Network Protocols (ICNP '06)*, Nov. 2006.
- [27] H. Li, Y. Cheng, C. Zhou, and P. Wan, "Multi-Dimensional Conflict Graph Based Computing for Optimal Capacity in MR-MC Wireless Networks," *Proc. Int'l Conf. Distributed Computing Systems (ICDCS '10)*, June 2010.
- [28] M.R. Garey and D.S. Johnson, *Computers and Intractability: A Guide to the Theory of NP-Completeness*. W.H. Freeman & Co., 1990.
- [29] K. Jain, J. Padhye, V.N. Padmanabhan, and L. Qiu, "Impact of Interference on Multi-Hop Wireless Network Performance," *Proc. ACM MobiCom*, Sept. 2003.
- [30] H. So, A. Tkachenko, and R.W. Brodersen, "A Unified Hardware/Software Runtime Environment for FPGA Based Reconfigurable Computers Using Borph," *Proc. Int'l Conf. Hardware-Software Codesign and System Synthesis*, Oct. 2006.
- [31] J.H. Reed, *Software Radio: A Modern Approach to Radio Engineering*. Prentice Hall, May 2002.
- [32] Defense Advanced Research Projects Agency (DARPA), "The Next Generation Program (XG) Official Website," <http://www.darpa.mil/sto/smallunitops/xg.html>, 2012.
- [33] J. Tang, S. Misra, and G. Xue, "Joint Spectrum Allocation and Scheduling for Fair Spectrum Sharing in Cognitive Radio Wireless Networks," *Computer Networks J.*, vol. 52, no. 11, pp. 2148-2158, Aug. 2008.
- [34] Y.T. Hou, Y. Shi, and H.D. Sherali, "Spectrum Sharing for Multi-Hop Networking with Cognitive Radios," *IEEE J. Selected Areas in Comm.*, vol. 26, no. 1, pp. 146-155, Jan. 2008.
- [35] Y. Shi and Y.T. Hou, "A Distributed Optimization Algorithm for Multi-Hop Cognitive Radio Networks," *Proc. IEEE INFOCOM*, Apr. 2008.
- [36] M. Pan, C. Zhang, P. Li, and Y. Fang, "Joint Routing and Scheduling for Cognitive Radio Networks Under Uncertain Spectrum Supply," *Proc. IEEE INFOCOM*, Apr. 2011.
- [37] L. Giupponi, R. Agusti, J. Perez-Romero, and O.S. Roig, "A Novel Approach for Joint Radio Resource Management Based on Fuzzy Neural Methodology," *IEEE Trans. Vehicular Technology*, vol. 57, no. 3, pp. 1789-1805, May 2008.
- [38] G. Ganesan and Y.G. Li, "Cooperative Spectrum Sensing in Cognitive Radio: Part I: Two User Networks," *IEEE Trans. Wireless Comm.*, vol. 6, pp. 2204-2213, June 2007.
- [39] H. Kim and K.G. Shin, "Efficient Discovery of Spectrum Opportunities with MAC-Layer Sensing in Cognitive Radio Networks," *IEEE Trans. Mobile Computing*, vol. 7, no. 5, pp. 533-545, May 2008.
- [40] W.-Y. Lee and I.F. Akyildiz, "Optimal Spectrum Sensing Framework for Cognitive Radio Networks," *IEEE Trans. Wireless Comm.*, vol. 7, no. 10, pp. 3845-3857, Oct. 2008.
- [41] P. Gupta and P.R. Kumar, "The Capacity of Wireless Networks," *IEEE Trans. Information Theory*, vol. 46, no. 2, pp. 388-404, Mar. 2000.
- [42] Y. Shi, Y.T. Hou, and S. Kompella, "How to Correctly Use the Protocol Interference Model for Multi-Hop Wireless Networks," *Proc. ACM MobiHoc*, May 2009.

- [43] C. Gao, Y. Shi, Y.T. Hou, H.D. Sherali, and H. Zhou, "Multicast Communications in Multi-Hop Cognitive Radio Networks," *IEEE J. Selected Areas in Comm.*, vol. 29, no. 4, pp. 784-793, Apr. 2011.
- [44] J. Tang, G. Xue, and W. Zhang, "Interference-Aware Topology Control and QoS Routing in Multi-Channel Wireless Mesh Networks," *Proc. ACM MobiHoc*, May 2005.
- [45] Y. Pochet and L.A. Wolsey, *Production Planning by Mixed Integer Programming*, Operations Research and Financial Engineering, Springer-Verlag, 2006.
- [46] IBM ILOG CPLEX Optimizer, <http://www-01.ibm.com/software/integration/optimization/cplex-optimizer>, 2012.
- [47] R. Diestel, *Graph Theory*. Springer, 2005.
- [48] A. Raniwala and T. cker Chiueh, "Architecture and Algorithms for An IEEE 802.11-Based Multi-Channel Wireless Mesh Network," *Proc. IEEE INFOCOM*, Mar. 2005.



Miao Pan received the BSc degree in electrical engineering from the Dalian University of Technology, China, in 2004, the MSc degree in electrical and computer engineering from the Beijing University of Posts and Telecommunications, China, in 2007, and the PhD degree in electrical and computer engineering from the University of Florida in 2012. He is now an assistant professor in the Department of Computer Science at Texas Southern University. His

research interests include cognitive radio communications and networking, wireless security and network economics, and resource management in cyber-physical systems such as wireless sensor networks, cloud computing, and smart grids. He is a member of the IEEE.



Hao Yue received the BSc degree in telecommunication engineering from Xidian University, China, in 2005. He has been working toward the PhD degree in the Department of Electrical and Computer Engineering at the University of Florida, Gainesville, since August 2009. His research interests include wireless network coding, RFID protocol design, and cross-layer optimization. He is a student member of the IEEE.



Chi Zhang received the BE and ME degrees in electrical engineering from the Huazhong University of Science and Technology, Wuhan, China, in July 1999 and June 2002, respectively, and the PhD degree in electrical and computer engineering from the University of Florida in August 2011. He is now an associate professor in the School of Information Science and Technology, University of Science and Technology of China, Hefei. His current research

interests include network and distributed system security, wireless networking, and mobile computing. He is a member of the IEEE.



Yuguang Fang received the PhD degree in systems engineering from Case Western Reserve University in January 1994 and the PhD degree in electrical engineering from Boston University in May 1997. He was an assistant professor in the Department of Electrical and Computer Engineering at the New Jersey Institute of Technology from July 1998 to May 2000. He joined the Department of Electrical and Computer Engineering at the University of

Florida in May 2000 as an assistant professor, then got an early promotion to an associate professor with tenure in August 2003 and to a full professor in August 2005. He held a University of Florida Research Foundation (UFRF) Professorship from 2006 to 2009, a Changjiang Scholar Chair Professorship with Xidian University, Xi'an, China, from 2008 to 2011, and a Guest Chair Professorship with Tsinghua University, China, from 2009 to 2012. He has published more than 300 papers in refereed professional journals and conferences. He received the US National Science Foundation Faculty Early Career Award in 2001, the US Office of Naval Research Young Investigator Award in 2002, the Best Paper Award from the IEEE International Conference on Network Protocols (ICNP) in 2006, and the IEEE TCGN Best Paper Award from the IEEE High-Speed Networks Symposium at IEEE GlobeCom in 2002. He also received a 2010-2011 UF Doctoral Dissertation Advisor/Mentoring Award, a 2011 Florida Blue Key/UF Homecoming Distinguished Faculty Award, and the 2009 UF College of Engineering Faculty Mentoring Award. He is also active in professional activities. He is currently serving as the editor-in-chief for *IEEE Transactions on Vehicular Technology*. He served as the editor-in-chief for *IEEE Wireless Communications* (2009-2012) and serves/ served on several editorial boards of technical journals, including *IEEE Transactions on Mobile Computing* (2003-2008, 2011-present), *IEEE Transactions on Communications* (2000-present), *IEEE Transactions on Wireless Communications* (2002-2009), *IEEE Journal on Selected Areas in Communications* (1999-2001), *IEEE Wireless Communications Magazine* (2003-2009), and *ACM Wireless Networks* (2001-present). He served on the steering committee for *IEEE Transactions on Mobile Computing* (2008-2010). He actively participates in professional conference organizations, such as serving as the technical program cochair for IEEE INFOCOM (2014), steering committee cochair for QShine (2004-2008), technical program vice-chair for IEEE INFOCOM (2005), technical program area chair for IEEE INFOCOM (2009-2013), technical program symposium cochair for IEEE GlobeCom (2004), and member of technical program committee for IEEE INFOCOM (1998, 2000, 2003-2008). He is a fellow of the IEEE and the IEEE Computer Society and a member of the ACM.

► For more information on this or any other computing topic, please visit our Digital Library at www.computer.org/publications/dlib.